MOLECULAR PHYSICS, 1984, VOL. 51, NO. 4, 887–906

On the rovibrational levels of the H_3^+ and H_2D^+ molecules

by JONATHAN TENNYSON
Science & Engineering Research Council, Daresbury Laboratory,
Daresbury, Warrington WA4 4AD, England

and BRIAN T. SUTCLIFFE
Department of Chemistry, University of York,
Heslington, York YO1 5DD, England

(*Received* 18 *July* 1983 ; *accepted* 11 *October* 1983)

Variationally exact rovibrational levels for the H_3^+ and H_2D^+ molecules are calculated using a recently published accurate potential. Vibrational fundamentals are $\nu_{A_1}=3191$ cm^{-1} and $\nu_E=2494$ (2521·6) cm^{-1} for H_3^+ and $\nu_1=3000$ cm^{-1}, $\nu_2=2184$ cm^{-1} and $\nu_3=2310$ cm^{-1} for H_2D^+. For H_3^+ calculated ground state rotational constants are $B_0=43{\cdot}51$ (43·57) cm^{-1}, $C_0=20{\cdot}59$ (20·71) cm^{-1}, $D_J{}^0=0{\cdot}04$ (0·05) cm^{-1}, $D_{JK}{}^0=-0{\cdot}07$ ($-0{\cdot}10$) cm^{-1} and $D_K=0{\cdot}04$ (0·04) cm^{-1} (where experimental results are given in parenthesis). An attempt is made to stabilize many vibrational states. We thus reassess the results of Carney and Porter. The implications for astrophysics, the interpretation of the infrared spectrum of H_3^+ near its dissociation limit and the unassigned spectrum of H_2D^+ are discussed.

1. INTRODUCTION

The H_3^+ molecular ion and its isotopic variants (HD_2^+, H_2D^+, D_3^+ etc.) are the simplest known polyatomic molecules from the point of view of electronic structure. The vibration–rotation spectra of these systems are of considerable consequence in astrophysics [1, 2]. H_3^+ and HD_2^+ have been the subject of extensive experimental investigation by Carrington *et al.* [3], who observed more than 26 000 transitions arising from molecules near their dissociation limit. These results are as yet unexplained. Infrared vibration–rotation spectra have been reported for H_3^+ by Oka [4] and for D_3^+ [5] and H_2D^+ [6] by Shy and co-workers. The H_2D^+ spectrum remains unassigned.

The simplicity of the systems means that it is possible to calculate *ab initio* and with high accuracy their rotation–vibration spectra, assuming that electronic and nuclear motions are separable. There are many highly accurate electronic potential energy surfaces available in the literature for these systems [7–11] and it is thus possible to concentrate on *ab initio* calculation of the vibration–rotation structure.

The vibration–rotation spectra of these systems have been studied extensively by Carney and Porter [12–16] in a series of very detailed and careful papers. The potential energy surface used by these authors [9] was however variationally inferior to several [8, 10, 11] that are now available and they used one of a family of conventional methods of vibrational analysis based on the Eckart hamiltonian

[17]. In the work reported here one of the improved potential energy surfaces is used and the vibration–rotation problem is solved by a method that does not depend on any equilibrium-geometry assumptions as for the Eckart method. In this way it is hoped to reassess the results of Carney and Porter, to elucidate certain of the astrophysical implications of the spectra of the systems and to further the understanding of the infrared results of Carrington *et al.* [3]. We also discuss the possibility of assigning the H_2D^+ spectrum of Shy *et al.* [6].

The potential energy surface used in this work is that of Schinke, Dupuis and Lester [11] which, besides giving energies about 200 cm^{-1} below those of the Carney and Porter surface [9], is easily the most extensive of the accurate surfaces available, based as it is on CI calculations at 650 different geometries.

The vibration–rotation hamiltonian used is one that has proved extremely satisfactory in earlier work by the authors on systems as diverse as KCN [18], H_2Ne [18], HeHF [19] and CH_2^+ [20, 21]. It is particularly appropriate for systems that can be thought of as formed by atom–diatom collisions and which undergo large amplitude internal motions. It is thus suitable for the present investigations, both in view of the probable way in which the systems are formed and in view of the fact that the light H atoms can be expected to vibrate with much larger amplitudes than would be found in near-rigid systems. Recent work by the authors [18–22] and by Carter and Handy [21, 23, 24] has shown the danger of using the Eckart hamiltonian in such circumstances.

2. THE VIBRATION ROTATION HAMILTONIAN

It was shown in [18] that if a triatomic molecule was considered as an atom (1), H or D, colliding with a diatom (2–3), H_2, then the hamiltonian for internal motion could be written in terms of the space-fixed coordinates $\mathbf{t}_i$ with

$$\left.\begin{aligned} \mathbf{t}_1 &= \mathbf{x}_1 - \mathbf{x}_d, \\ \mathbf{t}_2 &= \mathbf{x}_3 - \mathbf{x}_2, \end{aligned}\right\} \tag{1}$$

as

$$\hat{H}^t = -\frac{\hbar^2}{2\mu}\nabla^2(\mathbf{t}_1) - \frac{\hbar^2}{2\mu_d}\nabla^2(\mathbf{t}_2) + V. \tag{2}$$

In these equations the $\mathbf{x}_1$ represent the laboratory-fixed coordinates of the nuclei with

$$\mathbf{x}_d = m_d^{-1}(m_2\mathbf{x}_2 + m_3\mathbf{x}_3) \tag{3}$$

and

$$\left.\begin{aligned} \mu^{-1} &= m_1^{-1} + m_d^{-1}, \\ \mu_d^{-1} &= m_2^{-1} + m_3^{-1}. \end{aligned}\right\} \tag{4}$$

The transformation inverse to (1) above is

$$\left.\begin{aligned} \mathbf{x}_1 &= \mathbf{X} + M^{-1}m_d\mathbf{t}_1, \\ \mathbf{x}_2 &= \mathbf{X} - m_1M^{-1}\,\mathbf{t}_1 - m_3m_d^{-1}\,\mathbf{t}_2, \\ \mathbf{x}_3 &= \mathbf{X} - m_1M^{-1}\,\mathbf{t}_1 + m_2m_d^{-1}\,\mathbf{t}_2, \end{aligned}\right\} \tag{5}$$

where $\mathbf{X}$ is the centre-of-nuclear mass coordinate, M is the sum of the nuclear masses and m_d is $(m_2 + m_3)$.

In [18] a body-fixed coordinate system was introduced by means of an orthogonal matrix $\mathbf{C}$ such that

$$\mathbf{t}_i = \mathbf{C}\mathbf{z}_i \tag{6}$$

with $\mathbf{C}$ defined by choosing

$$\mathbf{z}_1 = \begin{pmatrix} 0 \\ 0 \\ R \end{pmatrix}, \quad \mathbf{z}_2 = r \begin{pmatrix} \sin\theta \\ 0 \\ \cos\theta \end{pmatrix}. \tag{7}$$

Here R is the length of $\mathbf{t}_1$, r the length of $\mathbf{t}_2$ and θ the angle between $\mathbf{t}_1$ and $\mathbf{t}_2$. This choice corresponds to choosing a body-fixed coordinate system in which the z-axis is along $\mathbf{t}_1$ with θ in the range $(0, \pi)$ so that the diatomic system lies in the positive half of the xz-plane.

The hamiltonian expressed in this coordinate system is then

$$H = \hat{K}_{\mathrm{V}} + \hat{K}_{\mathrm{VR}} + V(R, r, \theta) \tag{8}$$

where

$$\hat{K}_{\mathrm{V}} = \frac{-\hbar^2}{2\mu R^2}\frac{\partial}{\partial R}\left(R^2\frac{\partial}{\partial R}\right) - \frac{\hbar^2}{2\mu_{\mathrm{d}} r^2}\frac{\partial}{\partial R}\left(r^2\frac{\partial}{\partial R}\right) - \frac{\hbar^2}{2}\left(\frac{1}{\mu R^2}\right) + \frac{1}{\mu_{\mathrm{d}} r^2}\frac{1}{\sin\theta}\frac{\partial}{\partial\theta}\left(\sin\theta\frac{\partial}{\partial\theta}\right), \tag{9}$$

$$\hat{K}_{\mathrm{VR}} = \tfrac{1}{2}\left[\frac{1}{\mu R^2}(\Pi_x^2 + \Pi_y^2) + \left(\frac{\cot^2\theta}{\mu R^2} + \frac{\operatorname{cosec}^2\theta}{\mu_{\mathrm{d}} r^2}\right)\Pi_z^2 + \frac{\cot\theta}{\mu R^2}(\Pi_x\Pi_z + \Pi_z\Pi_x)\right] + \frac{\hbar}{i}\frac{1}{\mu R^2}\left(\frac{\partial}{\partial\theta} + \frac{\cot\theta}{2}\right)\Pi_y. \tag{10}$$

The jacobian for integral evaluation in this coordinate system is just $R^2 r^2 \sin\theta$. The Π_α are components of the total angular momentum and, as explained in [18], are chosen to satisfy the normal commutation relations. They are functions of the Euler angles δ, γ and ϵ only and they represent the angular momentum of the system.

In this work, as previously [18–20], a basis set of nuclear motion functions is used, which is essentially composed of product functions of the form

$$\psi_{n,m}(r, R)\theta_{jk}(\theta)D_{Mk}{}^{J}(\delta, \gamma, \epsilon), \tag{11}$$

where $\psi_{n,m}$ is a function of the internal radial coordinates, θ_{jk} is a standard associated Legendre polynomial [25] and $D_{Mk}{}^{J}$ is a rotation matrix element (symmetric top function) in the convention of Brink and Satchler [26]. The acronym LC–RAMP (linear combination of radial and angular momentum products) has been coined for this approach [27].

In fact, for reasons discussed in the Appendix (see also [18]), it is always possible to choose symmetrized angular functions of the form

$$\left.\begin{aligned} &2^{1/2}[\theta_{jk}(\theta)D_{Mk}{}^{J}(\delta, \gamma, \epsilon) + (-1)^p\theta_{j-k}(\theta)D_{M-k}{}^{J}(\delta, \gamma, \epsilon)], && p = 0, 1;\ k > 0, \\ &\theta_{j0}(\theta)D_{M0}{}^{J}(\delta, \gamma, \epsilon), && p = 0;\ k = 0. \end{aligned}\right\} \tag{12}$$

Following convention [28], the $p = 0$ functions are labelled e and $p = 1$ functions f.

If $\hat{H}$ is allowed to operate from the left on the angular functions (12) and the result multiplied from the left by their complex conjugate, integrating over all angular coordinates gives an effective hamiltonian for the radial coordinates [18]. This is usually known as the close-coupling hamiltonian [29]. In order for the angular integration discussed above to be analytic, it is necessary to express the potential in the form

$$V(r, R, \theta)=\sum_{\lambda=0}^{\Lambda} P_\lambda(\cos\theta)V_\lambda(r, R). \tag{13}$$

This can be done for an arbitrary potential by performing $(\Lambda+2)$ point Gauss–Legendre integration in θ for each (r, R) point of interest as explained in [20] (see also [30]). Providing Λ is chosen large enough this entails no loss of accuracy. When the diatomic part is homonuclear, as here, only terms with λ even appear in (13).

For the H_3^+ potential of Schinke *et al.* [8] the use of $\Lambda=30$ was found to give a very accurate representation of the surface. Care only needed to be taken with the representation of the nuclear singularities at $R=r/2$. All the calculations reported here used $\Lambda=30$; tests showed that the results are insensitive to larger expansions.

The radial basis functions are chosen here, as previously [18–20], to be of the form

$$\psi_{n,m}(r, R)=r^{-1}\, H_n(r)R^{-1}\, H_m(R). \tag{14}$$

For the diatomic-like radial coordinate we have found functions based on Morse oscillators to be appropriate

$$\left.\begin{aligned} H_n(y)&=\beta^{1/2}\, N_{n\alpha} \exp(-y/2)y^{(\alpha+1)/2}\, L_n^{\alpha}(y),\\ y&=A\exp[-\beta(r-r_e)], \end{aligned}\right\} \tag{15}$$

where $N_{n\alpha}L_n^{\alpha}$ is a normalized Laguerre polynomial [31] and r_e is the equilibrium value of r. A and β can be related to the dissociation energy, D_e, and fundamental vibrational frequency, ω_e, of the appropriate pseudodiatomic Morse curve

$$A=\frac{4D_e}{\hbar\omega_e},\quad \beta=\omega_e\left(\frac{\mu_d}{2D_e}\right)^{1/2} \tag{16}$$

and α is the integer closest to A. In practice r_e, D_e and ω_e are optimized variationally to give the best basis set expansion for a particular problem.

For the R coordinate we have previously used both Morse oscillator-like functions and functions based on spherical oscillators [32]

$$\left.\begin{aligned} H_m(y)&=N_{m\eta}y^{(\eta+1)/2}\exp(-\eta/2)L_m^{\eta+1/2}(y),\\ y&=\xi R^2, \end{aligned}\right\} \tag{17}$$

where ξ equals $(\mu\omega_e)^{1/2}$ with ω_e equal to the fundamental R stretching frequency. Again η and ω_e are optimized for each problem.

As observed by ter Haar [33], the Morse oscillator-like functions do not obey the correct boundary conditions at $x=0$ (where x is r or R) and can only be used if the wavefunctions have effectively vanished at this limit. This is not a limitation on the spherical oscillator functions and such functions have been used successfully in earlier work [20] to describe motions that have large amplitude at $R=0$. Trial functions composed of both types of functions are used in the present work since it is at least possible that quasi-linear configurations of the system are important at high energy. The calculations reported here were performed with programs ATOMDIAT [34] and ATOMDIAT2 [30]. We refer to these for details of the numerical procedures used. Program GENPOT [30] was used for the numerical Legendre expansion of the potential. All calculations were performed on the CRAY-1 at Daresbury Laboratory.

We note that (as established in the Appendix) the functions (11) used in these calculations are adapted to be a basis for irreducible representations of the permutation group of order 2 (S_2). They are not, however, adapted to be a basis for S_3. Thus the full permutation symmetry of the H_2D^+ problem is automatically reflected in the chosen basis, but that of the H_3^+ problem is not. In the Appendix it is established that functions with even and functions with odd j respectively form bases for the two different irreducible representations of S_2. Since S_2 is a sub-group of S_3 this symmetry distinction will persist in S_3. In both the H_2D^+ and H_3^+ problems, therefore, the secular equations will split into four parts, corresponding to the p parity (e or f see equation (12)) and the j parity (even or odd). When $J=0$, p can only be e so that here there is only a twofold splitting.

The precise permutational symmetries in the H_3^+ problem are of central importance in determining the nuclear spin statistics of the problem and detailed discussion of appropriate assignments is given in the Appendix.

So far we have not specified the form of the potential in detail. However if the electronic Born–Oppenheimer potential were to be used directly, then it would belong to the totally symmetric representation of S_3. In practice the potential is fitted and though from the fitting (see [11]) it may be ascertained that the potential has the correct symmetry for $R<4\ a_0$, it is possible that at greater distances this is not accurately the case.

3. Calculations with $J=0$

For a non-linear molecule, such as H_3^+, a calculation with $J=0$ is sufficient to define the vibrational states of the system. In H_3^+ itself, of course, nuclear spin statistics dictate that these $J=0$ levels are never actually occupied (see Appendix).

We started by optimizing a basis for the *diatomic* coordinate r for an isolated H_2 molecule. Basis functions for the scattering coordinate R were then obtained by optimizing for H_3^+ with r frozen at its equilibrium separation, $1{\cdot}65\ a_0$. Contrary to our previous experience [19], the basis set obtained in this fashion was found to give a poor representation of H_3^+. The diatomic r functions in particular were found to be inadequate and could only be improved by optimizing them for a full H_3^+ calculation. The diatomic H_2 functions were particularly poor at representing the higher vibrational states supporting the impression gained during this work that the higher vibrational states of H_3^+/H_2D^+ do not behave like H_2 and H^+/D^+, as was suggested by Carrington *et al.* [3].

As we were interested in a broad range of vibrational states, we decided to optimize the basis sets by focusing on the 40th $J=0$ level of a calculation with j

Table 1. Vibrational ($J=0$) energy levels for H_3^+ in cm^{-1}. All energies are relative to the dissociation limit of H_2+H^+. The calculations used basis functions with $n \leqslant 7$, $m \leqslant 10$ and $j \leqslant 19$ and for the diatomic r basis, $r_e=2{\cdot}1\ a_0$, $D_e=45\ 000\ \text{cm}^{-1}$ and $\omega_e=2590\ \text{cm}^{-1}$. The states are numbered from the lowest level upwards for each parity of j.

	j even			j odd	
	Morse†	Spherical‡		Morse†	Spherical‡
1	−32580·48	−32580·48			
2	−30086·1	−30086·1	1	−30086.22	−30086·22
3	−29389·4	−29389·4			
4	−27855·5	−27855·5			
5	−27622·3	−27622·2	2	−27622·5	−27622·5
6	−27035·2	−27035·2	3	−27035·6	−27035·6
7	−26303·7	−26303·7			
8	−25635·1	−25635·6	4	−25637·2	−25637·2
9	−25344·4	−25345·2			
			5	−25129·2	−25129·2
10	−24840·2	−24840·2			
			30	−18056	−18055
40	−18483	−18455			

† Morse oscillator-like functions of equation (15) with $R_e=1{\cdot}71\ a_0$, $D_e=50\ 500\ \text{cm}^{-1}$ and $\omega_e=1866\ \text{cm}^{-1}$.

‡ Spherical oscillator-like functions of equation (17) with $\eta=8{\cdot}05$ and $\omega_e=6145\ \text{cm}^{-1}$.

Table 2. Vibrational ($J=0$) energy levels for H_2D^+ in cm^{-1}. All energies are relative to the dissociation limit of H_2+H^+. The calculations used basis functions with $n \leqslant 7$, $m \leqslant 10$ and $j \leqslant 19$ and for the diatomic r basis, $r_e=2{\cdot}1\ a_0$, $D_e=45\ 000\ \text{cm}^{-1}$ and $\omega_e=2590\ \text{cm}^{-1}$. The states are numbered from the lowest level upwards for each parity of j.

	j even			j odd	
	Morse†	Spherical‡		Morse†	Spherical‡
1	−32962·30	−32962·29	1	−30652·57	−30652·57
2	−30778·3	−30778·3	2	−28537·4	−28537·3
3	−29962·4	−29962·4	3	−27729·4	−27729·4
4	−28717·0	−28716·9	4	−26617·2	−26617·2
5	−28398·2	−28398·2	5	−26195·4	−26195·4
6	−27937·2	−27936·9			
7	−27074·5	−27074·4	30	−19410	−19405
8	−26725·0	−26725·0			
9	−26361·8	−26361·9			
10	−25997·7	−25997·2			
40	−19952	−19940			

† Morse oscillator-like functions of equation (15) with $R_e=1{\cdot}71\ a_0$, $D_e=50\ 500\ \text{cm}^{-1}$ and $\omega_e=1866\ \text{cm}^{-1}$.

‡ Spherical oscillators with $\eta=9{\cdot}80$ and $\omega_e=5926\ \text{cm}^{-1}$.

even. Test calculations showed that the parity of j used in basis set optimization calculations was unimportant. Tables 1 and 2 present results for optimized H_3^+ and H_2D^+ calculations respectively. These calculations were performed with large basis sets, 880 functions, in an attempt to converge as many vibrational states as possible, although it was clear that the low-lying levels could be satisfactorily represented by a much smaller calculation (see § 4).

Tables 1 and 2 show excellent agreement between calculations perfomed with different R basis functions. Both calculations clearly converged to the same limit and no problems were encountered with the domain of the Morse-like functions. However, the functions based on Morse oscillators were found to perform consistently better than those based on spherical oscillators. This can be attributed to the extra flexibility of the three adjustable parameters which allow, in particular, the functions to be shifted to an appropriate R_e. These Morse oscillator-like functions were thus used for all calculations with $J > 0$.

Convergence checks on the results of tables 1 and 2 showed that whilst the lower states were well converged (1 cm^{-1} or better), the high-lying states were still poorly represented at this level of calculation. The 40th j even state, for example, is only converged to about 100 cm^{-1}. As this state lies less than half way to dissociation, direct calculations on the *near dissociation* states observed by Carrington *et al.* [3] were deemed impractical.

However, even at this binding energy the spacing between vibrational states is only 140 cm^{-1} in H_3^+ and 120 cm^{-1} in H_2D^+ (and might be decreased by a better calculation). This spacing will be even lower in the near dissociation region. This region will thus contain a very dense and complicated manifold of vibrational states which would almost certainly be chaotic in the sense of classical trajectory calculations [35]. If this is the case, a small change in the calculation (either through the potential or the basis set) can be expected to impart a large perturbation to the calculated spectrum. Such perturbations give rise to a web of avoided crossings [36]. Current quantum mechanical methods cannot yet cope with this complicated stochastic behaviour in real potentials.

Because, as explained above, the basis functions used are not adapted to S_3, it is not possible to assign, *a priori*, symmetry designations to the states of H_3^+ shown in table 1. In the Appendix it is established that, if a state is non-degenerate, then, if j is even, it is a basis function for the totally symmetric representation of S_3 and if j is odd then it is a basis function for the antisymmetric (alternating) representation of S_3. If there are a pair of degenerate states, one with j even and the other with j odd, then they form a basis for the two dimensional irreducible representation of S_3. Because C_{3v} is isomorphic with S_3 it is possible to label these representations by their C_{3v} designation. Thus if the state is non-degenerate then it may be labelled A_1 if j is even or A_2 if j is odd. The degenerate states may be labelled E. This labelling is convenient because it enables the present results to be put into correspondence with results calculated in a conventional way, based on an equilibrium geometry. It should be remembered, however, that no such conventional assumption is made in the present calculations.

Given that the basis functions used are not adapted to S_3, then the degeneracy of certain solutions is not built into the calculations from the start. But if the set of basis functions is sufficiently complete, it should turn out that certain of the solutions are degenerate to within computational accuracy. Table 1 is laid out in such a way as to indicate where it is believed that these degeneracies lie, in some of the lower energy states of the system. For the reasons outlined above, these degeneracies will be very difficult to identify in the higher energy states of the system. However the presence of convincing degeneracies in the lower lying states would seem to indicate that for these states the present calculations are well converged and that the extent of the basis function set is adequate.

It should be noticed too, that although the fitted potential of Schinke *et al.* [11] may not be fully symmetric for $R > 4\,a_0$, this apparently has little effect on the low-lying states.

Table 3. The zero point energy and ten lowest vibrational band origins of H_3^+ in cm^{-1}.

Quantum numbers				CP	Carney	
ν_{A_1}	ν_E	l	Symmetry	[14, 15]	[15]	This work
0	1	1	E	2515·99 2516·17	2545·99	2494·3† 2494·4
1	0	0	A_1	3185·32	3220·48	3191·1
0	2	0	A_1	4799·19	4864·82	4725·0
0	2	2	E	5004·13	5050·99	4958·0 4958·3
1	1	1	E	5567·81	5622·35	5544·9 5545·3
2	0	0	A_1	6267·77	6334·18	6276·8
0	3	1	E	7123·07	7210·07	6943·3 6944·4
0	3	3	A_1	7441·85	7505·21	7235·0
0	3	3	A_2	7515·61	7565·56	7451·3
1	2	0	A_1	7821·21	7906·80	7740·3
E_0				4345·19		4327·7

† Experimental result 2521·56 ± 0·14 [4].

Table 4. Zero point energy and ten lowest vibrational band origins of H_2D^+ in cm^{-1}.

Quantum numbers			CP	
ν_1	ν_2	ν_3	[13]	This work
0	1	0	2203	2184·0
0	0	1	2329	2309·7
1	0	0	3000	2999·9
0	2	0	4314	4245·3
0	1	1	4490	4424·9
0	0	2	4605	4564·1
1	1	0	5067	5025·1
1	0	1	5264	5232·9
2	0	0	5888	5887·8
0	3	0	6430	6236·4
E_0			3963·0 [16]	3945·9

Tables 3 and 4 give our calculated band origins and zero point energies for H_3^+ and H_2D^+. Those obtained by Carney and Porter (CP) [13–16] are given for comparison. The only relevant experimental observation is the infrared measurement of the degenerate bending fundamental by Oka [4]. The theoretical results agree with this result to within 1 per cent (the better agreement by CP with their less accurate surface must be regarded as fortuitous).

The agreement between our calculations and those of CP is very good for the stretching fundamentals and overtones (especially for H_2D^+, where it is exact). For the bending modes our results are consistently lower than those of CP for both systems. In comparing results one must remember that not only do the vibrational basis sets differ, but also the potential energy surfaces upon which the calculations are based. This makes a direct comparison difficult. Our results suggest that the surface of Schinke *et al.* [11] is flatter in the bending coordinate than the surfaces of CP [9, 15]. Also, the comparatively large discrepancies in the higher bending modes (100–200 cm^{-1} for the second bending overtones compared with 20 cm^{-1} for the bending fundamentals) suggest that these states are not fully converged in the CP calculations.

Although our zero point energies are lower than those of CP, the differences nearly cancel between H_3^+ and H_2D^+ so that we obtain essentially the same energy differences as they do for the exchange reaction

$$H_3^+ + HD \rightleftharpoons H_2D^+ + H_2. \tag{18}$$

However, a complete understanding of this reaction requires knowledge of states with $J > 0$ which are considered in the following section.

4. CALCULATIONS WITH $J > 0$

The low-lying rotational states of H_3^+ and H_2D^+ are of major interest in astrophysics as they determine the equilibrium in reactions such as (18). In particular, they are important because of the observed over-abundance, due to fractionation [2], of molecules containing (rare) heavy isotopes (for example D, ^{13}C, ^{15}N, ^{18}O) in interstellar clouds. Whilst for astrophysics the lowest allowed states are of primary importance, in order to understand laboratory infrared spectra a range of rotational states must be considered.

In general, the size of the basis needed for a rovibrational calculation grows linearly with J, unless the so-called off-diagonal Coriolis interactions are neglected [18–20]. Neglect of these terms proved to be a poor approximation for H_3^+. It was important, therefore, for us to optimize small basis sets to represent the vibrational ground states, so as to keep the problem tractable. We optimized basis sets with $m \leqslant 4$, $n \leqslant 4$ and $j \leqslant 15$ to represent the ground states of H_3^+ and H_2D^+. Table 5 shows the convergence of the H_3^+ basis for the lowest $J = 0 \rightarrow 1^e$ transition. This transition is never actually observed as the $J = 0$ state is spin forbidden. Indeed the $J = 1^e$ state is the ground state of H_3^+. Clearly the small ($m \leqslant 4$, $n \leqslant 4$ and $j \leqslant 14$) basis is very well converged for this transition.

Table 6 presents energy levels for H_3^+ rotational states up to $J = 4$, in both the ground and first excited vibrational states. The rotational levels have been labelled so as to identify the basis set symmetries used in each calculation (note that k is not actually a good quantum number). They have also been labelled

Table 5. Convergence of the lowest $J=1^{\mathrm{e}}$ state and of the lowest $J=0\rightarrow 1^{\mathrm{e}}$ transition frequency for H_3^+ in cm^{-1}. The basis set used Morse-like functions with $r_{\mathrm{e}}=1{\cdot}71\ a_0$, $D_{\mathrm{e}}=22\ 000$ cm^{-1} and $\omega_{\mathrm{e}}=2590$ cm^{-1} for r, and $R_{\mathrm{e}}=1{\cdot}68\ a_0$, $D_{\mathrm{e}}=57\ 000$ cm^{-1} and $\omega_{\mathrm{e}}=2410$ cm^{-1} for R.

$m^{\max}$	$n^{\max}$	$j^{\max}$	$J=1^{\mathrm{e}}$	$J=0\rightarrow 1^{\mathrm{e}}$
4	4	14	−32516·386	64·047
6	4	14	−32516·394	
4	6	14	−32516·438	
4	4	18	−32516·386	
5	8	16	−32516·446	64·048

Table 6. Low-lying rotational states of H_3^+ relative to the $J=0$ state at −32 580·433 cm^{-1} for the ground state and −30 083·8 cm^{-1} for the first ($\nu_E=1$) excited state. The calculations used basis sets with $m\leqslant 4$, $n\leqslant 4$ and $j\leqslant 15$ basis of table 5.

			Ground state		Excited state			
J	K	k	j†	Frequency/ cm^{-1}	j†	Frequency/ cm^{-1}	j†	Frequency/ cm^{-1}
1	0	1^{f}	o	86·870	o	88·1	e	85·8
	1	0^{e}	e	64·047	e	25·7	o	25·8
	1	1^{e}	o	64·048	o	93·6	e	104·8
2	1	2^{f}	e	237·095	e	257·9	o	290·8
	1	1^{f}	o	237·090	o	201·5	e	201·9
	2	0^{e}	e	169·083	e	92·0	o	92·1
	2	1^{e}	o	169·081	o	231·0	e	282·4
	0	2^{e}	e	259·615	e	269·0	o	267·4
	0	3^{f}	o	516·296	o	542·6	e	541·6
3	2	2^{f}	e	427·520	e	478·3	o	479·5
	2	1^{f}	o	427·520	o	354·8	e	355·6
	3	0^{e}	e	314·945	e	197·7	o	197·5
	3	1^{e}	o	314·927	o	407·5	e	407·4
	1	2^{e}	e	494·202	e	470·5	o	470·9
	1	3^{e}	o	494·207	o	502·0	e	566·2
4	1	4^{f}	e	832·593	e	831·2	o	1030·0
	1	3^{f}	o	832·598	o	830·4	e	822·9
	3	2^{f}	e	657·853	e	735·9	o	735·5
	3	1^{f}	o	657·923	o	547·5	e	547·7
	4	0^{e}	e	501·376	e	342·5	o	342·2
	4	1^{e}	o	501·356	o	620·9	e	620·7
	2	2^{e}	e	767·568	e	710·3	o	712·1
	2	3^{e}	o	767·559	o	800·5	e	802·5
	0	4^{e}	e	854·140	e	903·2	o	902·6

† Parity of j in the basis : e = even, o = odd.

by the conventional symmetric-top label K [37], which has been assigned on the basis of the calculated energy ordering. We have not distinguished between levels which differ by the sign of K.

Again, although our basis set does not have the full symmetry of the H_3^+ problem, converged results should reflect the full symmetry of the system.

For a non-degenerate vibrational state, such as ground state H_3^+, states with $K=1$, 2 and 4 are of E symmetry and this is apparent in our results. States with $K=3$ are only pseudo-degenerate [37] and show larger splittings. It is customary to fit these rotational levels with perturbation-type hamiltonians [38]. Table 7 compares our results with those obtained experimentally by Oka [4]. The agreement is very good. With these parameters it is possible to predict higher J states for H_3^+.

Table 7. Comparison of calculated and experimental rotational constants in cm^{-1} for the vibrational ground state of H_3^+.

	Experiment	Calculated	
	Oka [4]	CP†	This work
B	43·568 ± 0·048	43·3223	43·507
C	20·708 ± 0·048	20·565	20·589
D_J	0·047 ± 0·007		0·040
D_{JK}	−0·099 ± 0·018		−0·071
D_K	0·040 ± 0·003		0·035

† Quoted by Oka [4]. Carney also calculated $B=43{\cdot}62$ cm^{-1} [16].

For a degenerate vibrational state, such as the first excited state of H_3^+, the situation is more complicated. The states with $K=0$ should form, on the conventional analysis, a rigorously degenerate pair for j even and odd, for all J. Similarly, the states with $K=3$ should form two degenerate pairs for all values of J. Since our results for the rotational levels of the first state are not as well converged as for those of the ground state, this degeneracy is less well reflected but still apparent. For states with $K=1$, 2 and 4 there should be one pair of properly degenerate states with E symmetry and a pair of states, A_1 and A_2, which may be nearly degenerate. In H_3^+ the A_1 states are nuclear spin forbidden. Our $K=1$ results can easily be assigned into degenerate (for example J, $k=1$, 0^e) and non-degenerate (J, $k=1$, 1^e) pairs on energetic grounds. For the $K>1$ levels such assignments are not practical on energetic grounds alone.

These rotational levels can also be fitted to perturbation-type hamiltonians. For example, the term due to $\xi=-1$ [37] can easily be detected in our results. A complete fitting, however, would require representing the Coriolis terms in the fashion of Alieve and Watson [39]. We did not feel our results were accurate enough to warrant such treatment.

Table 8 gives the results of calculations on the low-lying levels of H_2D^+ in its ground and first excited vibrational states. The rotational levels have been labelled by J_τ as H_2D^+ is a highly asymmetric top with $\kappa \simeq -0{\cdot}07$.

Table 8. Low-lying rotational states of H_2D^+ relative to the $J=0$ ground state at $-32\,962{\cdot}259$ cm^{-1} and (0, 1, 0) state at $-30\,776{\cdot}6$ cm^{-1}. The calculations used basis sets with $m \leqslant 4$, $n \leqslant 4$ and $j \leqslant 15$, Morse-like functions with $r_e = 1{\cdot}71\ a_0$, $D_e = 22\,000$ cm^{-1} and $\omega_e = 2590$ cm^{-1} for r, and $R_e = 1{\cdot}65\ a_0$, $D_e = 47\,200$ cm^{-1} and $\omega_e = 1964$ cm^{-1} for R.

				Ground state	(0, 1, 0) state
J	τ	k	j†	Frequency/cm^{-1}	Frequency/cm^{-1}
1	+1	1^f	o	72·369	72·5
	−1	0^e	e	45·634	40·6
	0	1^e	o	59·958	52·6
2	+1	2^f	e	218·417	209·2
	0	1^f	o	175·702	173·3
	−2	0^e	e	131·461	111·9
	−1	1^e	o	138·665	116·1
	+2	2^e	e	223·610	221·1
3	+3	3^f	o	459·318	450·1
	0	2^f	e	354·344	332·9
	−1	1^f	o	325·711	314·0
	−3	0^e	e	251·055	208·8
	−2	1^e	o	253·689	209·7
	+1	2^e	e	375·865	374·3
	+2	3^e	o	457·837	399·9
4	+3	4^f	e	777·799	648·7
	+2	3^f	o	653·699	647·3
	−1	2^f	e	530·652	491·8
	−2	1^f	o	515·435	484·0
	−4	0^e	e	402·310	332·9
	−3	1^e	o	403·080	333·2
	0	2^e	e	580·699	566·1
	+1	3^e	o	644·782	566·7
	+4	4^e	e	778·136	584·3

† Parity of j in the basis : e = even, o = odd.

Selection rules for the infrared transition of H_2D^+ with our notation are $\Delta J = 0$, ± 1 with the parity, $J+p$, changed and the parity of j conserved. Table 9 gives frequencies for P, Q and R transitions from states up to $J=3$ for the lowest vibrational fundamental. These were computed using $\nu_2 = 2184{\cdot}0$ cm^{-1} (see table 4).

These results may be compared with the unassigned spectrum of Shy *et al.* [6]. Even when allowance is made for a possible 1 per cent error in ν_2 (20 cm^{-1}), it is apparent that there is no correspondence between the levels in table 9 and the observed transitions. This suggests that the experimental spectrum arises from rotational levels with $J > 3$, which would form the upper range of the levels suggested by Shy *et al.* However, we hope that our results might assist in the assigning of lower temperature observations. Consideration of the partition

Table 9. Calculated rotational structure of the ν_2 fundamental of H_2D^+ for initial $J \leqslant 3$.

(J	k) → (J'	k')	j†	Frequency/cm^{-1}	(J	k) → (J'	k')	j†	Frequency/cm^{-1}
3	3^f	2	1^e	o	1842·3	3	2^f	3	3^e	o	2229·6
3	3^f	2	1^f	o	1898·0	1	1^f	3	2^e	o	2232·6
3	2^e	2	0^e	e	1920·1	3	1^e	2	1^e	e	2240·1
3	3^f	3	0^e	o	1933·4	1	0^e	3	1^f	e	2246·1
2	2^e	1	0^e	e	2001·0	2	0^e	2	0^e	o	2246·9
3	2^e	2	2^e	e	2029·2	2	1^e	2	2^f	o	2250·3
3	1^f	2	1^f	o	2031·6	3	1^e	3	1^e	e	2254·5
3	2^e	2	2^f	e	2038·8	2	2^e	3	3^f	e	2255·0
3	2^f	3	1^e	e	2039·3	3	0^e	3	0^e	o	2258·2
3	0^e	2	0^e	e	2044·9	3	1^e	3	2^f	o	2261·3
3	1^e	2	1^e	o	2046·4	3	1^e	4	1^e	o	2263·3
3	3^e	3	2^f	o	2059·1	1	0^f	4	0^e	e	2263·5
3	3^e	4	1^e	o	2059·3	3	1^e	2	1^f	o	2265·8
2	1^f	3	0^e	o	2067·0	2	3^f	4	3^e	o	2284·0
2	1^f	1	1^f	e	2080·8	3	2^f	3	2^f	e	2292·9
2	2^e	2	1^e	e	2081·7	2	2^f	3	2^f	e	2298·5
2	0^e	1	0^e	e	2093·2	2	1^e	3	1^f	o	2321·4
3	1^e	1	1^e	o	2097·0	3	2^f	3	2^f	e	2322·3
2	3^f	3	2^e	o	2098·0	1	1^e	4	1^e	o	2334·7
3	1^f	2	0^e	e	2120·2	1	0^e	2	2^e	e	2359·4
2	2^e	3	1^f	e	2122·1	3	3^f	4	3^f	o	2372·0
1	2^e	2	1^f	e	2133·7	3	2^e	4	2^e	e	2374·2
3	0^e	0	0^e	e	2738·4	3	0^e	3	3^f	e	2382·0
1	2^e	4	0^e	o	2141·0	3	2^e	4	4^e	e	2392·5
3	1^f	1	0^e	e	2152·3	2	0^e	3	2^e	e	2426·8
2	0^e	2	2^e	e	2154·0	2	1^e	3	3^e	o	2445·2
3	2^e	3	0^e	o	2169·1	2	1^f	3	3^f	o	2458·4
1	3^f	4	1^f	e	2208·7	3	2^f	4	4^f	e	2478·4
0	0^e	1	1^f	e	2210·9	3	1^e	4	3^e	o	2497·0
2	0^e	1	0^e	e	2224·6	3	0^e	4	2^e	e	2499·0
2	0^e	2	1^f	o	2225·9	3	1^f	4	3^f	o	2505·6
3	1^f	2	2^e	e	2229·4	3	0^e	4	4^e	e	2517·3

† Parity of j : e = even, o = odd.

function (see below) shows that the transition frequencies shown in table 9 will dominate a spectrum recorded below 100 K.

The partition function for a system within the electronic Born–Oppenheimer approximation is defined as

$$z = \sum_i g_i \exp(-E_i/kT), \tag{19}$$

where the energies are those of the nuclear motion states and the g_i their statitical weights. At low temperatures it is sufficient to consider only the rotational states

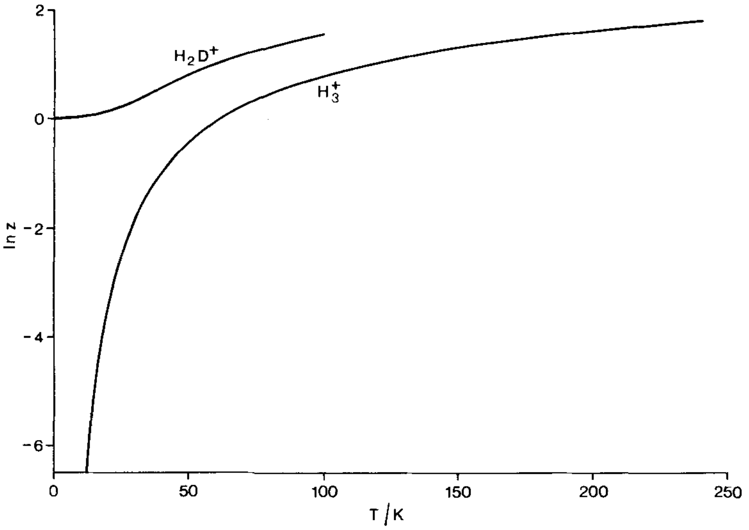

Logarithms of the partition functions as a function of temperature for H_3^+ and H_2D^+.

of the lowest vibrational level. (The ν_E state for H_3^+ makes a significant contribution to the partition function only above 250 K.) The g_i are determined by the nuclear spin statistics as identified in the Appendix.

The figure shows the calculated partition functions for H_3^+ and H_2D^+ as a function of temperature. It should be noticed that we have used the lowest $J=0$ states as the energy base. Thus for H_3^+, $z \to 0$ as $T \to 0$.

Finally our best value for the ground state energy of H_2D^+ is $-32\,962{\cdot}30$ cm^{-1} and for the lowest $J=1$ state of H_3^+ is $-32\,516{\cdot}45$ ($-32\,580{\cdot}50$ cm^{-1} for the $J=0$ state). These figures confirm the theoretical values of $\Delta H_0^0/R = 136$ K used by Smith, Adams and Alge [2] for the isotope exchange reaction (18).

5. Conclusion

In this work we have calculated the rovibrational levels of H_3^+ and H_2D^+ using an accurate potential energy surface. These results enable us to reassess the extensive work of Carney and Porter [9, 12–17] on these systems. In general, we obtain good agreement.

We find significantly lower zero point energies than Carney and Porter for both H_3^+ and H_2D^+. However, this lowering is uniform and hence our zero point energy contribution to the predicted equilibrium constant of the isotope exchange reaction (18) agrees with the value derived by Smith *et al.* [2] from the results of Carney [16].

The energies of our bending fundamentals and overtones for H_3^+ and H_2D^+ are lower than those of Carney and Porter suggesting that the surface of Schinke *et al.* [11] is flatter in this coordinate than the surfaces used by Carney and Porter, and that the higher bending overtones reported by Carney and Porter may not be fully converged.

Experimental data on H_3^+ and H_2D^+ is limited. However, we obtain good agreement with the results of Oka [4] for H_3^+. In particular, the agreement with his rotational levels is excellent. Both the agreement with the calculations of Carney and Porter, and that with the experiments of Oka is particularly gratifying as we make no assumptions whatsoever about equilibrium structure.

The vibrational spectrum of H_3^+ (and H_2D^+) near dissociation proved too dense to be easily amenable to this sort of variational approach. Its density suggest that the levels are probably chaotic.

We thank Dr. Reinhard Schinke for supplying a copy of his H_3^+ potential energy surface and Dr. David Clary and Dr. David Smith for drawing our attention to the astrophysical significance of the system.

APPENDIX

The laboratory-fixed hamiltonian is invariant under all rotation-reflections and under all permutations of identical particles. The space-fixed hamiltonian (2) is similarly invariant but, because of the coordinate change $\mathbf{x}_i \rightarrow \mathbf{t}_i$, the permutational invariance may be obscured. In the body-fixed hamiltonian this invariance may be even further obscured by the choice of internal coordinates and can in general result in mixing of the two parts of the hamiltonian H_V and H_{VR} (see for example (8)). In this Appendix we consider these problems for our internal coordinate system.

Let it be supposed that the transformation from the laboratory-fixed coordinates to the space fixed coordinates is written

$$\mathbf{X} = M^{-1} \sum_{i=1}^{N} m_i \mathbf{x}_i, \tag{A 1}$$

$$\mathbf{t}_i = \sum_{j=1}^{N} V_{ij} \mathbf{x}_j \tag{A 2}$$

and its inverse written as

$$\mathbf{x}_i = \mathbf{X} + \sum_{j=1}^{N-1} \tilde{V}_{ij} \mathbf{t}_j. \tag{A 3}$$

Here $\mathbf{X}$ is the centre of mass and M the total mass of the system. $\mathbf{V}$ and $\tilde{\mathbf{V}}$ are constant matrices. (A 2) is exemplified by (1) in the text and (A 3) by (5).

If a permutation P is realized on the $\mathbf{x}_i$ so that

$$\mathbf{x}_i \rightarrow \mathbf{x}'_i = \sum_{j=1}^{N} P_{ij} \mathbf{x}_j, \tag{A 4}$$

where $\mathbf{P}$ is a standard orthogonal permutation matrix, then the same permutation is realized on $\mathbf{t}_i$ by

$$\mathbf{t}_i \rightarrow \mathbf{t}'_i = \sum_{j=1}^{N-1} (\mathbf{V}\mathbf{P}\tilde{\mathbf{V}})_{ij} \mathbf{t}_j = \sum_{j=1}^{N-1} H_{ij} \mathbf{t}_j. \tag{A 5}$$

If the permutation involves only identical particles then $\mathbf{X}$ is invariant. Such invariance will be assumed from now on.

In the special case of three particles of identical masses it is easily established from (1) and from (5) that

$$\mathbf{V}=\begin{pmatrix}1 & -1/2 & -1/2\\ 0 & -1 & 1\end{pmatrix},\quad \tilde{\mathbf{V}}=\begin{pmatrix}2/3 & 0\\ -1/3 & -1/2\\ -1/3 & +1/2\end{pmatrix}. \tag{A 6}$$

Simple algebra then shows the following correspondences

$$\left.\begin{array}{cccc}
\mathbf{P} & 1\,(1)(2)(3) & 2\,(23) & 3\,(12)\\[4pt]
\mathbf{P} & \begin{pmatrix}1&0&0\\0&1&0\\0&0&1\end{pmatrix} & \begin{pmatrix}1&0&0\\0&0&1\\0&1&0\end{pmatrix} & \begin{pmatrix}0&1&0\\1&0&0\\0&0&1\end{pmatrix}\\[4pt]
\mathbf{H} & \begin{pmatrix}1&0\\0&1\end{pmatrix} & \begin{pmatrix}1&0\\0&-1\end{pmatrix} & \begin{pmatrix}-1/2&-3/4\\-1&1/2\end{pmatrix}\\[4pt]
\mathbf{P} & 4\,(13) & 5\,(132) & 6\,(123)\\[4pt]
\mathbf{P} & \begin{pmatrix}0&0&1\\0&1&0\\1&0&0\end{pmatrix} & \begin{pmatrix}0&0&1\\1&0&0\\0&1&0\end{pmatrix} & \begin{pmatrix}0&1&0\\0&0&1\\1&0&0\end{pmatrix}\\[4pt]
\mathbf{H} & \begin{pmatrix}-1/2&3/4\\1&1/2\end{pmatrix} & \begin{pmatrix}-1/2&3/4\\-1&-1/2\end{pmatrix} & \begin{pmatrix}-1/2&-3/4\\1&-1/2\end{pmatrix}
\end{array}\right\} \tag{A 7}$$

If the particles 2 and 3 alone are permuted then only the first two matrices are relevant.

The matrices $\mathbf{H}$ of (A 7) provide a faithful but non-orthogonal representation of S_3, which may be shown to be equivalent to the standard representation $\{21\}$ (or E in C_{3v} notation).

The space-fixed coordinates $\mathbf{t}_i$ are related to the body-fixed coordinates and the Euler angles by (6) supplemented by three accessory conditions which may be written generally as

$$f_m(\mathbf{C}^T(\mathbf{t})\mathbf{t}_i)=0, \quad m=1, 2, 3 \tag{A 8}$$

and are exemplified by the vanishing elements in (7).

The constraint relations (A 8) define the elements of $\mathbf{C}$ as functions of the $\mathbf{t}_i$ and, once $\mathbf{C}$ is so determined, the relation (6) defines the $\mathbf{z}_i$ and hence the body-fixed internal coordinates. Given that the $\mathbf{z}_i$ have been expressed as functions of the $\mathbf{t}_i$ then (A 8) can be rewritten as the set of functional identities

$$f_m(\mathbf{z}_i)=0, \quad m=1, 2, 3. \tag{A 9}$$

The effect of a permutation $\mathbf{t}\to\mathbf{Ht}$ on the definition of $\mathbf{C}$ can be obtained from (A 8) by writing the induced change as

$$f_m\left(\bar{\mathbf{C}}^T(\mathbf{t})\sum_{j=1}^{N-1} H_{ij}{}^{-1}\,\mathbf{t}_j\right)=0,\quad \bar{\mathbf{C}}(\mathbf{t})=\mathbf{C}(\mathbf{H}^{-1}\,\mathbf{t}),\quad m=1,2,3. \tag{A 10}$$

By virtue of the orthogonality requirement, $\bar{\mathbf{C}}(\mathbf{t})$ is another orthogonal matrix and so, on the same assumptions that lead to (A 9), the induced change in $f_m(\mathbf{z}_i)$ is

$$f_m\left(\sum_{j=1}^{N-1} H_{ij}{}^{-1}\,\bar{\mathbf{z}}_j\right)=0,\quad m=1,2,3, \tag{A 11}$$

with

$$\bar{\mathbf{z}}_j=\bar{\mathbf{C}}\mathbf{t}_j. \tag{A 12}$$

But (A 11) and (A 9) are functional identities so it follows that

$$\mathbf{z}_i=\sum_{j=1}^{N-1} H_{ij}{}^{-1}\,\bar{\mathbf{z}}_j \tag{A 13}$$

and, using (A 12), that

$$\mathbf{t}_j=\mathbf{C}\sum_{j=1}^{N-1} H_{ji}\bar{\mathbf{z}}_i. \tag{A 14}$$

Comparing (A 14) with (6) it is seen that the transformation induced by the permutation is just

$$\mathbf{z}_j\to\bar{\mathbf{z}}'_j=\mathbf{F}\sum_{j=1}^{N-1} H_{ji}\mathbf{z}_i,\quad \mathbf{F}=\mathbf{C}^T\bar{\mathbf{C}}. \tag{A 15}$$

The orthogonal matrix $\mathbf{F}$ will in general be a function not only of the Euler angles but of the internal coordinates too. It can be regarded as transforming the body-fixed frame. The transformed internal coordinates are generated from the permuted $\mathbf{z}_i$ just as the original internal coordinates are generated from the $\mathbf{z}_i$ themselves.

It should be clear from the above discussion that, unless $\mathbf{F}$ and the permuted $\mathbf{z}_i$ are reasonably simply related to $\mathbf{C}$ and to the original $\mathbf{z}_i$ respectively, then the changes induced in the function space built on the Euler angles and the internal coordinates will be too complicated to be of any practical use in the formation of symmetry functions. In the present case it turns out that only the permutation P_2 has usefully simple properties. To see this, imagine $\mathbf{t}_1$ expressed in polar form as (R,γ,δ) and $\mathbf{t}_2$ likewise as (r,α,β). Standard matrix algebra on (7) then shows that γ and δ are two of the Euler angles and $\epsilon=\beta-\delta$ is the third. This is as indicated in the designation of $D_{Mk}{}^J$ in (11). The internal coordinates R and r are just the moduli of $\mathbf{t}_1$ and $\mathbf{t}_2$ (and hence $\mathbf{z}_1$ and $\mathbf{z}_2$) respectively and, again by standard algebra

$$\begin{aligned}\cos\theta&=\cos\alpha\cos\gamma+\sin\alpha\sin\gamma\cos\epsilon\\&=\mathbf{z}_1{}^T\mathbf{z}_2/rR.\end{aligned} \tag{A 16}$$

If the permutation P_5 is considered then after a fair amount of tedious algebra it is possible to establish that, for example

$$R^2\to(R^2+\tfrac{9}{4}r^2+3rR\cos\theta)/4=R'^2 \tag{A 17}$$

and

$$C_{zz} \rightarrow -(C_{zx}\tfrac{3}{4}r \sin \theta + C_{zy}\tfrac{3}{4}r \cos \theta + C_{zz}R/2)/R', \qquad \text{(A 18)}$$

which are obviously unpromising expressions from the point of view of practical function manipulation.

If the permutation P_2 is considered however then it is easily established that $\theta \rightarrow \pi - \theta$, $\epsilon \rightarrow \pi + \epsilon$ and that r, R, γ and δ are invariant. (In this case $\mathbf{F}$ is a constant matrix.) The only induced functional changes relevant to (11) are then easily found. They are

$$\theta_{jk}(\theta) \rightarrow \theta_{jk}(\pi - \theta) = (-1)^{j+k}\theta_{jk}(\theta) \qquad \text{(A 19)}$$

and

$$D_{Mk}{}^{J}(\delta, \gamma, \epsilon) \rightarrow D_{Mk}{}^{J}(\delta, \gamma, \pi + \epsilon) = (-1)^{k} D_{Mk}{}^{J}(\delta, \gamma, \epsilon). \qquad \text{(A 20)}$$

The radial functions are invariant.

Thus the functions of the form (11) are split into two subsets, the set with j even which do not change sign under P_2 and the set with j odd which do. The first set are the basis functions for $\{2\}$ of S_2 and the second set for $\{1^2\}$. (Since S_2 is isomorphic with C_V the designations A_1 and A_2 may be used if desired.)

Before considering how S_2 can be used to classify the representations of S_3, it is appropriate to consider the inversion symmetry to establish that it introduces no complications. The inversion symmetry of planar systems requires somewhat delicate consideration because the three constraint relations (A 8) are not independent in the planar case. Thus the relations (7) actually define only the $\hat{e}_z$ and $\hat{e}_x$ axes. The $\hat{e}_y$ axis is chosen subsequently to make the system right handed. (For a more detailed discussion see Ezra [40].) In the present case the inversion is realized on the $\mathbf{t}_i$ by the change $\mathbf{t}_i \rightarrow -\mathbf{t}_i$ and it follows that r, R, θ and ϵ are invariant while $\gamma \rightarrow \pi - \gamma$, $\delta \rightarrow \pi + \delta$. Thus the change induced in the functions (11) is

$$D_{Mk}{}^{J}(\delta, \gamma, \epsilon) \rightarrow D_{Mk}{}^{J}(\pi + \delta, \pi - \gamma, \epsilon) = (-1)^{J} D_{M-k}{}^{J}(\delta, \gamma, \epsilon). \qquad \text{(A 21)}$$

The inversion has therefore no implications for j and the form of (12) follows at once from (A 21).

Now from the theory of the symmetric group (see for example Hammermesh [41]) it can be established that if functions form a basis for $\{3\}$ ($\equiv A_1$) in S_3 then in S_2 they can form a basis only for $\{2\}$. Similarly if functions form a basis for $\{1^3\}$ ($\equiv A_2$) in S_3 then in S_2 they can form a basis only for $\{1^2\}$. If functions form a basis for $\{21\}$ ($\equiv E$) in S_3 then they form a basis for either $\{2\}$ or $\{1^2\}$ in S_2 according to the row of $\{21\}$ to which they belong.

Now in the present case it has been established that the variables $\mathbf{t}_i$ themselves form a basis for a representation of S_3 and so functions of the $\mathbf{t}_i$ must be constructable to form a basis for S_3 too. It follows therefore that the function set (11), if sufficiently extensive, can form a basis for S_3. This and the discussions above justify the identifications made in § 3.

Consider now the nuclear spin multiplicity of the states, assuming that the identical particles are spin 1/2 fermions. Again standard theory (see for example Hammermesh [41]) establishes that for a total (space and spin) function to obey the Pauli principle, if the space part is a basis for a particular irreducible representation of the permutation group, then the spin part must be a basis for the conjugate representation. Thus, in the case of H_2D^+, the j-even states have a space part belonging to $\{2\}$ so the spin part must belong to $\{1^2\}$ and hence only triplet states will occur with j even. If j is odd then the spin part can only be $\{2\}$ and thus only singlet states occur with j odd. This is, of course, the classical ortho/para distinction and leads to a statistical weighting of 3 : 1 between the states. In the case of H_3^+ it is not possible to find a spin function basis for $\{1^3\}$ so that the states with j even belonging to $\{3\}$ ($\equiv A_1$) cannot occur and they have zero statistical weight. For states with j odd the spin part is $\{3\}$ and thus non-degenerate states with j odd are all quartets. For degenerate states the spin part is $\{21\}$ so that all degenerate states are doublets. Thus the statistical weight of a degenerate state is 2 and the statistical weight for a non-degenerate state with j odd is 4. These assignments of statistical weights lead to exactly the same weightings as are obtained using the conventional arguments as in [37].

REFERENCES

[1] HERBST, E., and KLEMPERER, W., 1976, *Physics Today*, **20**, 32.
[2] SMITH, D., ADAMS, N. G., and ALGE, E., 1982, *Astrophys. J.*, **263**, 123.
[3] CARRINGTON, A., BUTTENSHAW, J., and KENNEDY, R. A., 1982, *Molec. Phys.*, **45**, 753.
[4] OKA, T., 1980, *Phys. Rev. Lett.*, **45**, 531.
[5] SHY, J.-T., FARLEY, J. W., LAMB, W. E., JR., and WING, W. H., 1980, *Phys. Rev. Lett.*, **45**, 535.
[6] SHY, J.-T., FARLEY, J. W., and WING, W. H., 1980, *Phys. Rev.* A, **24**, 1146.
[7] CZISMADIA, I. G., KARI, R. E., POLANYI, J. C., ROACH, A. C., and ROBB, M. A., 1970, *J. chem. Phys.*, **52**, 6205.
[8] GIESE, C. F., and GENTRY, W. R., 1974, *Phys. Rev.* A, **10**, 2156.
[9] CARNEY, G. D., and PORTER, R. N., 1974, *J. chem. Phys.*, **60**, 4251.
[10] DYKSTRA, C. E., GAYLORD, A. S., GWINN, W. D., SWOPE, W. C., and SCHAEFFER III, H. F., 1978, *J. chem. Phys.*, **68**, 3951. DYKSTRA, C. E., and SWOPE, W. C., 1979, *J. chem. Phys.*, **70**, 1.
[11] SCHINKE, R., DUPUIS, M., and LESTER, W. A., JR., 1980, *J. chem. Phys.*, **72**, 3909.
[12] CARNEY, G. D., and PORTER, R. N., 1976, *J. chem. Phys.*, **65**, 3547.
[13] CARNEY, G. D., and PORTER, R. N., 1977, *Chem. Phys. Lett.*, **50**, 327.
[14] CARNEY, G. D., and PORTER, R. N., 1980, *Phys. Rev. Lett.*, **45**, 537.
[15] CARNEY, G. D., 1980, *Molec. Phys.*, **39**, 923.
[16] CARNEY, G. D., 1980, *Chem. Phys.*, **54**, 103.
[17] CARNEY, G. D., SPRANDEL, L. L., and KERN, C. W., 1978, *Adv. chem. Phys.*, **37**, 305.
[18] TENNYSON, J., and SUTCLIFFE, B. T., 1982, *J. chem. Phys.*, **77**, 4061.
[19] TENNYSON, J., and SUTCLIFFE, B. T., 1983, *J. chem. Phys.*, **79**, 43.
[20] TENNYSON, J., and SUTCLIFFE, B. T., 1983, *J. molec. Spectrosc.*, **101**, 71.
[21] CARTER, S., HANDY, N. C., and SUTCLIFFE, B. T., 1983, *Molec. Phys.*, **49**, 745.
[22] TENNYSON, J., and SUTCLIFFE, B. T., 1982, *Molec. Phys.*, **46**, 97.
[23] CARTER, S., and HANDY, N. C., 1982, *J. molec. Spectrosc.*, **95**, 9.
[24] CARTER, S., and HANDY, N. C., 1982, *Molec. Phys.*, **47**, 1445.
[25] CONDON, E. U., and SHORTLEY, G. H., 1935, *The Theory of Atomic Spectra* (Cambridge University).
[26] BRINK, D. M., and SATCHLER, G. R., 1968, *Angular Momentum*, 2nd edition (Clarendon).
[27] TENNYSON, J., and VAN DER AVOIRD, A., 1982, *J. chem. Phys.*, **77**, 5664.
[28] BROWN, J. M., HOUGEN, J. T., HUBER, K.-P., JOHNS, J. W. C., KOPP, I., LEFREBVRE-BRION, H., MERER, A. J., RAMSAY, D. A., ROSTOS, J., and ZARE, R. N., 1975, *J. molec. Spectrosc.*, **55**, 500.
[29] ARTHURS, A. M., and DALGARNO, A., 1960, *Proc. R. Soc.* A, **256**, 540.
[30] TENNYSON, J., 1984, *Comput. Phys. Commun.* (in the press).
[31] GRADSHTEYN, I. S., and RYZHIK, I. H., 1980, *Tables of Integrals, Series and Products* (Academic).
[32] MORSE, P. M., and FESHBACH, H., 1953, *Methods of Theoretical Physics*, Part II (McGraw-Hill), p. 1662.

[33] Ter Haar, D., 1946, *Phys. Rev.*, **70,** 222.
[34] Tennyson, J., 1983, *Comput. Phys. Commun.*, **29,** 307.
[35] Noid, D. W., Koszykowski, M. L., and Marcus, R. A., 1981, *A. Rev. phys. Chem.*, **32,** 267.
[36] Noid, D. W., Kozykowski, M. L., and Marcus, R. A., 1980, *Chem. Phys. Lett.*, **73,** 269.
[37] Herzberg, G., 1945, *Molecular Spectra and Molecular Structure II. Infrared and Raman Spectra of Polyatomic Molecules* (Van Nostrand), Chap. 1.
[38] Slawsky, Z. I., and Dennison, D. M., 1939, *J. chem. Phys.*, **7,** 509.
[39] Aliev, M. R., and Watson, J. K. G., 1976, *J. moec. Spectrosc.*, **61,** 29.
[40] Ezra, G. S., 1982, *Symmetry Properties of Molecules*, in Lecture Notes in Chemistry, edited by G. Berthier *et al.* (Springer-Verlag).
[41] Hammermesh, M., 1962, *Group Theory* (Addison-Wesley), Chap. 7.